21. ELEMENTAL PROFILE OF IRIDIUM AND OTHER ELEMENTS NEAR THE CRETACEOUS/TERTIARY BOUNDARY IN HOLE 577B[1]

Helen V. Michel and Frank Asaro, Lawrence Berkeley Laboratory
Walter Alvarez, University of California, Berkeley
and
Luis W. Alvarez, Lawrence Berkeley Laboratory[2]

ABSTRACT

An Ir anomaly of 61 ng/cm^2 was found in Deep Sea Drilling Project Hole 577B at the same stratigraphic level as the Cretaceous/Tertiary boundary defined by nannoplankton. This close correspondence supports the asteroid-impact theory for the Cretaceous/Tertiary boundary extinctions.

INTRODUCTION

An iridium anomaly associated with the Cretaceous/Tertiary boundary has been identified at more than 50 sites worldwide (Alvarez et al., 1984). The most viable explanation for this worldwide anomaly is that an asteroid or other extraterrestrial body about 10 km in diameter impacted the Earth 65 m.y. ago, exploded, and distributed a dust cloud of terrestrial and extraterrestrial material which encircled the Earth and settled in a few months. Samples from Hole 577B were examined using neutron-activation analysis (NAA) to test this prediction and to search for other geochemical anomalies that would shed light on the mechanisms of boundary deposition.

A single core containing seven sections and a core catcher was taken at Hole 577B and an intact Cretaceous/Tertiary boundary was recovered. The sediment is an undeformed white to light brown nannofossil ooze (see Site 577 chapter, this volume). The boundary region is light brown (in the midst of a slightly whiter region); this colored region extends from about Sample 577B-1-4, 58 cm to 577B-1-4, 72 cm. This boundary area is slightly firmer and more clay rich than the surrounding whiter regions.

METHODS

Continuous 1-cm samples were taken from 577B-1-4, 50 cm to 577B-1-4, 85 cm. Above and below this interval, spot samples were taken about every 5 cm. The sampling interval was increased farther from the boundary, eventually to a 50-cm interval in Sections 1 and 6 of Core 577B-1.

A total of 77 samples were first dried at 110°C and then measured by high-precision methods of NAA (Perlman and Asaro, 1969). Iridium was calibrated against the Danish boundary clay standard "DINO-1" (Alvarez et al., 1982a). Calcium was calibrated against a primary standard, $CaCO_3$. All other elements were calibrated against "Standard Pottery" (Perlman and Asaro, 1971).

The data from the NAA are shown in Table 1. The listed errors are one sigma values of the counting error or 1%, whichever is larger, and are about equal to the precision of measurement.

The iridium near the boundary (Samples 577B-1-4, 56 cm to 577B-1-4, 77 cm) could be measured precisely without any postirradiation chemistry. Farther from the boundary (as the level of Ir dropped), high temperature radiochemical separations were made in order to purify the Ir fraction without adding Ir carrier. In our procedure (which was inspired by the work of Rammensee and Palme, 1982) the same samples used for the regular NAA measurements (which each contained 100 mg of rock and 50 mg of cellulose binder) were heated to 1000°C in an oxidizing atmosphere to remove CO_2 and oxidizable carbon. The residues were then each mixed in a boron nitride crucible with 200 mg of powdered Fe, 100 mg of Hawaiian basalt (which served as a silicate flux), and a few milligrams of graphite (which provided a reducing environment). The crucibles (which were covered with a graphite plate) were slowly brought up to a temperature of 1477°C in a Deltech furnace under an argon atmosphere. The furnace was held at that temperature for 1 hr. and then slowly cooled. The slow speed was necessary to prevent the mulite dome, which permitted the controlled atmosphere, from fracturing.

The iron fraction in each crucible was in the form of a ball imbedded in a silicate glass. Each crucible was crushed, and the Fe ball was removed and then cleaned of residual glass with pliers. In the oxidizing firing step, the yield of Ir and other elements was 99 ± 1%. In the reduction firing step the yields were 100.0 ± 0.2, 99.85 ± 0.01, and 98.6 ± 0.2% for Ir, Co, and Fe radioactivities, respectively. Only 0.1 to 1% of the lithophile elements in the whole rock samples was extracted with the iron fraction.

This procedure provides a quantitative method of separating Ir radioactivity from the intense lithophile element radiations produced in NAA without adding Ir carrier, which can enhance the risk of laboratory contamination with Ir. The limits of detection for Ir were lowered to ~0.015 ppb for each sample, with a 1-day measurement time. As these low concentrations were considered to be background level Ir, four or more samples were analyzed simultaneously, resulting in a detection limit of 0.007 ppb in a 1-day measurement for highly calcareous samples.

RESULTS

Iridium Abundances

The Ir abundance profile at Hole 577B is plotted as a function of stratigraphic position in Figure 1. One major peak is seen (in Section 4), along with five smaller ones. To determine which of these peaks is most likely associated with an impacting meteorite and which with the normal iridium background resulting from meteorit-

[1] Heath, G. R., Burckle, L. H., et al., *Init. Repts. DSDP*, 86: Washington (U.S. Govt. Printing Office).
[2] Addresses: (Michel, Asaro, L. Alvarez) Lawrence Berkeley Laboratory, University of California, Berkeley, CA 94720; (W. Alvarez) Department of Geology and Geophysics, University of California, Berkeley, CA 94720.

Table 1. Elemental abundances in Core 577B-1.

Section	Interval (cm)	Al (%)	Ca (%)	Dy (ppm)	Mn (ppm)	U (ppm)	Ba (ppm)	Ir (ppb)	Cr (ppm)	Th (ppm)	Ni (ppm)	Tb (ppm)	Fe (%)
	10–11	0.33 ± 0.02	37.21 ± 0.83	9.22 ± 0.11	865 ± 9	0.241 ± 0.020	700 ± 18		2.2 ± 0.4	0.97 ± 0.03	21 ± 4	1.457 ± 0.044	0.25 ± 0.01
	50–51	0.31 ± 0.03	38.72 ± 0.88	8.95 ± 0.11	834 ± 8	0.232 ± 0.020	960 ± 21		6.0 ± 0.4	2.28 ± 0.03	29 ± 4	1.419 ± 0.043	0.24 ± 0.01
1	87–88	0.42 ± 0.04	40.51 ± 0.94	8.52 ± 0.11	897 ± 9	0.221 ± 0.019	884 ± 20	0.039 ± 0.008	3.8 ± 0.4	1.09 ± 0.03	25 ± 4	1.324 ± 0.041	0.26 ± 0.01
	100–101	0.21 ± 0.05	39.12 ± 0.95	7.09 ± 0.10	747 ± 7	0.193 ± 0.018	723 ± 18		2.4 ± 0.3	0.79 ± 0.03	21 ± 4	1.170 ± 0.036	0.20 ± 0.01
	140–141	0.46 ± 0.08	36.80 ± 0.99	13.73 ± 0.14	1104 ± 11	0.376 ± 0.023	656 ± 19		3.8 ± 0.4	1.24 ± 0.03	39 ± 5	2.273 ± 0.066	0.34 ± 0.01
	10–11	0.43 ± 0.02	36.70 ± 0.83	13.25 ± 0.13	1066 ± 11	0.294 ± 0.023	662 ± 19		3.4 ± 0.4	1.15 ± 0.03	32 ± 5	2.137 ± 0.063	0.31 ± 0.01
2	31–32	0.55 ± 0.03	37.82 ± 0.88	13.70 ± 0.15	1342 ± 13	0.339 ± 0.022	624 ± 19	0.073 ± 0.009	4.3 ± 0.4	1.37 ± 0.03	30 ± 5	2.179 ± 0.064	0.43 ± 0.01
	70–71	0.34 ± 0.04	37.43 ± 0.89	7.20 ± 0.10	707 ± 7	0.167 ± 0.017	514 ± 15		2.3 ± 0.3	0.72 ± 0.02	22 ± 4	1.165 ± 0.036	0.20 ± 0.01
	120–121	0.25 ± 0.05	35.78 ± 0.92	6.99 ± 0.10	718 ± 7	0.172 ± 0.017	528 ± 15		2.0 ± 0.3	0.58 ± 0.02	24 ± 4	1.076 ± 0.034	0.19 ± 0.01
	20–21	0.19 ± 0.06	38.40 ± 0.97	5.18 ± 0.08	241 ± 2	0.099 ± 0.016	312 ± 12		1.5 ± 0.3	0.40 ± 0.02	10 ± 3	0.783 ± 0.025	0.09 ± 0.01
	40–41	0.10 ± 0.02	38.86 ± 0.84	4.73 ± 0.07	181 ± 2	0.113 ± 0.015	358 ± 13		0.6 ± 0.3	0.29 ± 0.02	4 ± 3	0.737 ± 0.024	0.06 ± 0.01
	60–61	0.02 ± 0.02	37.24 ± 0.84	3.93 ± 0.06	124 ± 1	0.081 ± 0.014	350 ± 12		0.7 ± 0.2	0.26 ± 0.02	5 ± 3	0.627 ± 0.021	0.05 ± 0.01
3	80–81	0.08 ± 0.03	37.58 ± 0.87	5.12 ± 0.07	147 ± 1	0.109 ± 0.015	368 ± 13	0.016 ± 0.006	1.0 ± 0.3	0.35 ± 0.02	5 ± 3	0.820 ± 0.026	0.07 ± 0.01
	100–101	0.09 ± 0.05	37.59 ± 0.93	6.36 ± 0.08	233 ± 2	0.100 ± 0.017	229 ± 13		0.8 ± 0.3	0.49 ± 0.02	9 ± 3	1.038 ± 0.032	0.10 ± 0.01
	120–121	0.14 ± 0.06	37.48 ± 0.97	4.78 ± 0.07	177 ± 2	0.086 ± 0.016	335 ± 13		0.5 ± 0.3	0.36 ± 0.02	10 ± 3	0.787 ± 0.025	0.07 ± 0.01
	140–141	0.08 ± 0.02	38.21 ± 0.86	4.28 ± 0.07	195 ± 2	0.134 ± 0.016	157 ± 11		0.4 ± 0.2	0.34 ± 0.02	10 ± 3	0.709 ± 0.023	0.08 ± 0.01
	1–2	0.11 ± 0.02	38.98 ± 0.90	4.14 ± 0.07	156 ± 2	0.123 ± 0.015	270 ± 12		1.5 ± 0.2	0.30 ± 0.02	5 ± 3	0.633 ± 0.021	0.05 ± 0.01
	10–11	0.07 ± 0.03	38.79 ± 0.92	3.95 ± 0.06	118 ± 1	0.105 ± 0.015	328 ± 12	0.019 ± 0.006	1.0 ± 0.2	0.25 ± 0.02	6 ± 3	0.641 ± 0.021	0.05 ± 0.01
	20–21	0.12 ± 0.04	37.84 ± 0.94	3.98 ± 0.07	129 ± 1	0.082 ± 0.015	350 ± 12		0.4 ± 0.2	0.21 ± 0.02	5 ± 3	0.621 ± 0.021	0.04 ± 0.01
	30–31	0.14 ± 0.06	37.83 ± 0.99	3.58 ± 0.07	153 ± 2	0.079 ± 0.014	297 ± 11		0.6 ± 0.2	0.16 ± 0.02	9 ± 2	0.550 ± 0.019	0.04 ± 0.01
	35–36	0.04 ± 0.01	36.52 ± 0.86	3.58 ± 0.06	90 ± 1	0.098 ± 0.016	254 ± 11	0.058 ± 0.014	0.0 ± 0.2	0.35 ± 0.02	2 ± 2	0.512 ± 0.018	0.04 ± 0.01
	40–41	0.07 ± 0.01	38.51 ± 0.90	3.83 ± 0.08	137 ± 2	0.090 ± 0.014	267 ± 12	0.048 ± 0.007	0.6 ± 0.2	0.21 ± 0.02	8 ± 2	0.568 ± 0.018	0.03 ± 0.01
	45–46	0.04 ± 0.02	39.36 ± 0.92	3.98 ± 0.07	99 ± 1	0.080 ± 0.016	278 ± 11	0.117 ± 0.016	0.4 ± 0.2	0.13 ± 0.02	3 ± 2	0.555 ± 0.019	0.05 ± 0.01
	50–51	0.07 ± 0.01	39.01 ± 0.96	4.26 ± 0.08	89 ± 2	0.093 ± 0.013	339 ± 13	0.110 ± 0.014	0.3 ± 0.2	0.20 ± 0.02	1 ± 2	0.633 ± 0.020	0.04 ± 0.01
	51–52	0.04 ± 0.03	38.87 ± 0.95	4.51 ± 0.07	115 ± 1	0.085 ± 0.016	350 ± 13	0.194 ± 0.033	0.6 ± 0.3	0.25 ± 0.02	6 ± 3	0.585 ± 0.020	0.05 ± 0.01
	52–53	0.03 ± 0.04	38.35 ± 0.99	4.85 ± 0.07	117 ± 1	0.069 ± 0.016	457 ± 14	0.272 ± 0.029	1.2 ± 0.3	0.23 ± 0.02	14 ± 3	0.715 ± 0.024	0.06 ± 0.01
	53–54	0.10 ± 0.05	35.74 ± 0.99	4.40 ± 0.07	83 ± 1	0.080 ± 0.016	406 ± 13	0.166 ± 0.025	0.2 ± 0.3	0.17 ± 0.02	7 ± 3	0.648 ± 0.022	0.04 ± 0.01
	54–55	0.07 ± 0.01	36.87 ± 0.80	5.36 ± 0.07	136 ± 1	0.121 ± 0.017	541 ± 15	0.261 ± 0.023	1.3 ± 0.3	0.18 ± 0.02	8 ± 3	0.809 ± 0.026	0.08 ± 0.01
	55–56	0.11 ± 0.02	38.78 ± 1.00	5.36 ± 0.09	163 ± 2	0.096 ± 0.015	536 ± 16	0.443 ± 0.044	2.0 ± 0.3	0.21 ± 0.02	13 ± 3	0.849 ± 0.026	0.09 ± 0.01
	56–57	0.11 ± 0.02	37.88 ± 0.84	5.84 ± 0.07	164 ± 2	0.111 ± 0.018	629 ± 16	0.59 ± 0.05	2.0 ± 0.3	0.29 ± 0.02	15 ± 3	0.863 ± 0.028	0.11 ± 0.01
	57–58	0.10 ± 0.03	39.02 ± 0.89	6.19 ± 0.08	183 ± 2	0.109 ± 0.018	660 ± 16	0.83 ± 0.05	2.4 ± 0.3	0.35 ± 0.02	4 ± 3	0.901 ± 0.029	0.11 ± 0.01
	58–59	0.13 ± 0.04	39.77 ± 0.92	6.24 ± 0.08	191 ± 2	0.112 ± 0.018	712 ± 17	0.85 ± 0.04	3.3 ± 0.3	0.33 ± 0.02	9 ± 3	0.891 ± 0.029	0.12 ± 0.01
	59–60	0.17 ± 0.05	37.54 ± 0.94	6.34 ± 0.08	169 ± 2	0.104 ± 0.018	709 ± 17	1.21 ± 0.06	4.3 ± 0.3	0.31 ± 0.02	15 ± 3	0.961 ± 0.031	0.14 ± 0.01
	60–61	0.14 ± 0.03	37.88 ± 1.03	6.38 ± 0.10	215 ± 2	0.132 ± 0.016	779 ± 19	1.68 ± 0.07	4.9 ± 0.3	0.45 ± 0.02	19 ± 3	0.985 ± 0.029	0.19 ± 0.01
	61–62	0.20 ± 0.01	37.68 ± 0.79	6.66 ± 0.08	217 ± 2	0.097 ± 0.018	768 ± 17	1.95 ± 0.10	5.0 ± 0.3	0.48 ± 0.02	20 ± 3	1.001 ± 0.032	0.20 ± 0.01
	62–63	0.22 ± 0.02	38.31 ± 0.82	6.80 ± 0.08	232 ± 2	0.107 ± 0.017	792 ± 18	2.74 ± 0.12	6.3 ± 0.3	0.40 ± 0.02	20 ± 4	1.027 ± 0.033	0.24 ± 0.01
	63–64	0.28 ± 0.05	37.69 ± 1.08	6.50 ± 0.10	239 ± 2	0.140 ± 0.016	777 ± 19	3.05 ± 0.13	7.9 ± 0.3	0.47 ± 0.02	24 ± 3	1.049 ± 0.031	0.29 ± 0.01
	64–65	0.28 ± 0.02	36.26 ± 0.88	6.64 ± 0.09	230 ± 2	0.136 ± 0.016	834 ± 19	3.64 ± 0.16	12.0 ± 0.4	0.52 ± 0.02	33 ± 4	1.057 ± 0.031	0.38 ± 0.01
	65–66	0.28 ± 0.02	35.01 ± 0.90	6.80 ± 0.09	253 ± 3	0.123 ± 0.016	828 ± 19	4.55 ± 0.20	13.5 ± 0.4	0.63 ± 0.02	39 ± 4	1.106 ± 0.033	0.46 ± 0.01
	66–67	0.30 ± 0.03	36.30 ± 0.96	6.76 ± 0.09	248 ± 2	0.142 ± 0.017	762 ± 19	4.75 ± 0.19	15.0 ± 0.4	0.60 ± 0.02	43 ± 4	1.066 ± 0.032	0.50 ± 0.01
4	67–68	0.41 ± 0.05	35.35 ± 0.99	6.46 ± 0.09	285 ± 3	0.131 ± 0.016	697 ± 18	4.97 ± 0.21	15.0 ± 0.4	0.59 ± 0.02	31 ± 4	1.023 ± 0.031	0.48 ± 0.01
	68–69	0.35 ± 0.06	35.18 ± 1.02	6.43 ± 0.09	240 ± 2	0.133 ± 0.016	671 ± 17	4.96 ± 0.21	16.5 ± 0.4	0.62 ± 0.02	37 ± 4	0.977 ± 0.029	0.55 ± 0.01
	69–70	0.31 ± 0.01	36.59 ± 0.73	6.05 ± 0.08	230 ± 2	0.115 ± 0.016	523 ± 15	5.33 ± 0.21	22.8 ± 0.4	0.60 ± 0.02	42 ± 4	0.981 ± 0.030	0.54 ± 0.01
	70–71	0.33 ± 0.02	37.51 ± 0.80	5.63 ± 0.07	202 ± 7	0.121 ± 0.016	457 ± 14	5.61 ± 0.22	16.6 ± 0.4	0.55 ± 0.02	37 ± 4	0.912 ± 0.028	0.53 ± 0.01
	71–72	0.21 ± 0.02	34.30 ± 0.78	3.95 ± 0.06	135 ± 1	0.122 ± 0.014	272 ± 12	4.55 ± 0.18	12.1 ± 0.3	0.42 ± 0.02	28 ± 3	0.626 ± 0.021	0.39 ± 0.01
	72–73*	0.24 ± 0.03	35.84 ± 0.83	4.00 ± 0.06	125 ± 1	0.124 ± 0.014	245 ± 11	5.35 ± 0.21	18.5 ± 0.4	0.48 ± 0.02	36 ± 3	0.655 ± 0.021	0.46 ± 0.01
	73–74	0.24 ± 0.04	37.62 ± 0.88	3.86 ± 0.06	173 ± 2	0.086 ± 0.013	255 ± 11	2.50 ± 0.08	6.4 ± 0.3	0.26 ± 0.02	22 ± 3	0.593 ± 0.019	0.17 ± 0.01
	74–75	0.15 ± 0.01	38.51 ± 0.79	3.72 ± 0.06	115 ± 1	0.093 ± 0.014	247 ± 11	1.57 ± 0.05	4.0 ± 0.2	0.27 ± 0.02	10 ± 2	0.568 ± 0.018	0.10 ± 0.01
	75–76	0.07 ± 0.01	39.39 ± 0.82	3.23 ± 0.06	158 ± 2	0.062 ± 0.013	248 ± 10	0.670 ± 0.034	1.1 ± 0.2	0.21 ± 0.01	11 ± 2	0.477 ± 0.016	0.05 ± 0.01
	76–77	0.05 ± 0.02	38.79 ± 0.84	3.40 ± 0.06	102 ± 1	0.056 ± 0.013	185 ± 10	0.601 ± 0.036	0.4 ± 0.2	0.29 ± 0.02	7 ± 2	0.484 ± 0.016	0.04 ± 0.01
	77–78	0.10 ± 0.03	38.32 ± 0.88	3.50 ± 0.06	120 ± 1	0.090 ± 0.014	233 ± 11	1.07 ± 0.08	1.6 ± 0.2	0.21 ± 0.02	7 ± 2	0.537 ± 0.018	0.08 ± 0.01
	78–79	0.03 ± 0.04	37.21 ± 0.89	3.16 ± 0.06	108 ± 1	0.070 ± 0.013	234 ± 10	0.83 ± 0.08	1.9 ± 0.2	0.14 ± 0.01	7 ± 2	0.484 ± 0.016	0.05 ± 0.01
	79–80	0.03 ± 0.02	39.14 ± 0.86	3.07 ± 0.06	97 ± 1	0.045 ± 0.014	213 ± 10	0.465 ± 0.044	0.5 ± 0.2	0.19 ± 0.02	4 ± 2	0.473 ± 0.017	0.05 ± 0.01
	80–81	0.11 ± 0.03	37.83 ± 0.88	3.32 ± 0.06	123 ± 1	0.081 ± 0.014	289 ± 11	0.557 ± 0.050	0.5 ± 0.2	0.21 ± 0.02	5 ± 2	0.509 ± 0.018	0.04 ± 0.01
	81–82	0.10 ± 0.05	38.39 ± 0.91	3.50 ± 0.06	139 ± 1	0.095 ± 0.015	286 ± 10	0.87 ± 0.06	1.9 ± 0.2	0.20 ± 0.02	10 ± 2	0.536 ± 0.019	0.08 ± 0.01
	82–83	0.10 ± 0.01	41.23 ± 0.85	3.29 ± 0.06	140 ± 1	0.097 ± 0.015	291 ± 11	0.82 ± 0.06	2.3 ± 0.2	0.22 ± 0.02	10 ± 2	0.498 ± 0.018	0.07 ± 0.01
	83–84	0.12 ± 0.02	39.37 ± 0.85	3.25 ± 0.06	113 ± 1	0.100 ± 0.014	247 ± 10	0.53 ± 0.04	1.2 ± 0.2	0.24 ± 0.02	2 ± 2	0.476 ± 0.017	0.06 ± 0.01
	84–85	0.08 ± 0.02	40.38 ± 0.89	2.99 ± 0.06	118 ± 1	0.090 ± 0.014	224 ± 10	0.257 ± 0.030	0.7 ± 0.2	0.11 ± 0.02	5 ± 2	0.467 ± 0.017	0.04 ± 0.01
	85–86	0.05 ± 0.03	40.45 ± 0.92	2.98 ± 0.06	112 ± 1	0.054 ± 0.014	261 ± 10	0.229 ± 0.020	0.2 ± 0.2	0.16 ± 0.02	3 ± 2	0.446 ± 0.016	0.04 ± 0.01
	90–91	0.15 ± 0.04	38.89 ± 0.95	2.92 ± 0.05	90 ± 1	0.055 ± 0.014	236 ± 10	0.102 ± 0.013	0.7 ± 0.2	0.12 ± 0.02	4 ± 2	0.452 ± 0.016	0.03 ± 0.01
	100–101	0.10 ± 0.01		3.21 ± 0.06	105 ± 1	0.101 ± 0.012	259 ± 8	0.059 ± 0.011	0.4 ± 0.2	0.17 ± 0.01	3 ± 2	0.456 ± 0.014	0.03 ± 0.01
	110–111	0.11 ± 0.02		3.52 ± 0.06	126 ± 1	0.069 ± 0.012	312 ± 9	0.297 ± 0.025	1.2 ± 0.2	0.17 ± 0.01	7 ± 2	0.506 ± 0.015	0.06 ± 0.01
	120–121	0.14 ± 0.03		3.42 ± 0.06	117 ± 1	0.066 ± 0.012	289 ± 8		0.4 ± 0.2	0.22 ± 0.02	3 ± 2	0.493 ± 0.015	0.03 ± 0.01
	130–131	0.13 ± 0.04		3.34 ± 0.06	131 ± 1	0.083 ± 0.012	332 ± 9	0.019 ± 0.003	0.3 ± 0.2	0.13 ± 0.02	4 ± 2	0.503 ± 0.015	0.05 ± 0.01
	140–141	0.19 ± 0.05		3.54 ± 0.07	154 ± 2	0.099 ± 0.012	387 ± 9		0.8 ± 0.2	0.20 ± 0.02	4 ± 2	0.495 ± 0.015	0.04 ± 0.01
	150–151	0.13 ± 0.02		3.69 ± 0.06	158 ± 2	0.090 ± 0.012	310 ± 9		0.6 ± 0.2	0.21 ± 0.02	8 ± 2	0.506 ± 0.015	0.05 ± 0.01
	20–21	0.14 ± 0.03		3.90 ± 0.07	184 ± 2	0.079 ± 0.013	399 ± 9		0.6 ± 0.2	0.23 ± 0.02	4 ± 2	0.601 ± 0.017	0.05 ± 0.01
	40–41	0.08 ± 0.05		3.76 ± 0.07	176 ± 2	0.073 ± 0.013	368 ± 9		0.7 ± 0.2	0.24 ± 0.02	8 ± 2	0.528 ± 0.016	0.05 ± 0.01
	60–61	0.19 ± 0.07		3.73 ± 0.07	228 ± 2	0.064 ± 0.013	316 ± 9	0.012 ± 0.004	0.9 ± 0.2	0.23 ± 0.02	9 ± 3	0.554 ± 0.016	0.06 ± 0.01
5	80–81	0.29 ± 0.09		4.22 ± 0.07	293 ± 3	0.069 ± 0.012	524 ± 10		2.2 ± 0.2	0.26 ± 0.02	9 ± 3	0.589 ± 0.017	0.07 ± 0.01
	100–101	0.15 ± 0.01		4.62 ± 0.07	293 ± 3	0.098 ± 0.013	289 ± 8		1.0 ± 0.2	0.32 ± 0.02	11 ± 3	0.708 ± 0.019	0.06 ± 0.01
	120–121	0.75 ± 0.02		18.72 ± 0.21	2149 ± 21	0.362 ± 0.024	500 ± 14	0.14 ± 0.05	4.2 ± 0.4	1.33 ± 0.03	78 ± 6	3.416 ± 0.078	0.52 ± 0.01
	140–141	0.15 ± 0.02		5.48 ± 0.08	366 ± 4	0.086 ± 0.014	215 ± 8		1.0 ± 0.2	0.29 ± 0.02	14 ± 3	0.787 ± 0.021	0.08 ± 0.01
	30–31	0.12 ± 0.03		4.11 ± 0.07	209 ± 2	0.080 ± 0.013	426 ± 9		0.9 ± 0.2	0.24 ± 0.02	7 ± 2	0.628 ± 0.018	0.06 ± 0.01
6	48–49	0.16 ± 0.04		4.29 ± 0.07	240 ± 2	0.089 ± 0.013	442 ± 10	0.010 ± 0.006	0.7 ± 0.2	0.25 ± 0.02	10 ± 3	0.655 ± 0.018	0.06 ± 0.01
	90–91	0.18 ± 0.01		5.65 ± 0.08	363 ± 4	0.120 ± 0.014	323 ± 9		1.0 ± 0.2	0.31 ± 0.02	13 ± 3	0.861 ± 0.022	0.08 ± 0.01
	140–141	0.12 ± 0.01		4.17 ± 0.06	158 ± 2	0.072 ± 0.013	224 ± 8		0.6 ± 0.2	0.23 ± 0.02	4 ± 2	0.586 ± 0.017	0.04 ± 0.01

Note: Asterisk indicates location of Cretaceous/Tertiary boundary as determined by nannofossil biostratigraphy.

ic dust, the following model was used: During any brief interval of geological time, both the clay deposition rate and the Ir deposition rate from meteorite dust in the area of Hole 577B would be approximately constant. The rate of $CaCO_3$ deposition, however, could change as the biological productivity fluctuated or the calcite compensation depth varied. Changes in rates of $CaCO_3$ deposition would affect the abundances of clay and iridium, but not their ratios. For the present analysis, Fe rather than Al was taken as a measure of the clay abundance because Fe was measured with comparably high sensitivity throughout the section studied while Al was not.

Ir/Fe ratios are also shown in Figure 1. The background value is 2×10^{-8} in both the Cretaceous and Tertiary regions even though the Ir abundance varies by an order of magnitude. Thus, the broad Ir peak in Sections 1 and 2 (Peak E, Fig. 1) and the relatively sharp peak in Section 5 (Peak A, Fig. 1) may have been caused simply by changes in the deposition rate of $CaCO_3$. On the other hand, the main Ir peak and the three smaller

Table 1. (Continued).

Sm (ppm)	La (ppm)	Lu (ppm)	Co (ppm)	Sc (ppm)	Sb (ppm)	Eu (ppm)	Ce (ppm)	Hf (ppm)	Ta (ppm)	Yb (ppm)	Nd (ppm)
8.576 ± 0.086	34.76 ± 0.67	0.750 ± 0.019	10.15 ± 0.19	6.63 ± 0.07	0.17 ± 0.05	2.151 ± 0.022	18.28 ± 0.50	0.21 ± 0.04	0.043 ± 0.003	5.427 ± 0.054	40.1 ± 1.1
8.430 ± 0.084	34.56 ± 0.67	0.716 ± 0.018	10.49 ± 0.20	6.05 ± 0.06	0.26 ± 0.05	2.389 ± 0.024	18.68 ± 0.51	0.29 ± 0.04	0.038 ± 0.003	5.246 ± 0.053	40.3 ± 1.1
8.078 ± 0.081	33.15 ± 0.66	0.661 ± 0.017	11.46 ± 0.21	6.06 ± 0.06	0.22 ± 0.05	2.079 ± 0.021	19.75 ± 0.50	0.23 ± 0.04	0.044 ± 0.003	4.888 ± 0.051	39.0 ± 1.1
6.659 ± 0.067	27.98 ± 0.60	0.560 ± 0.015	8.95 ± 0.18	5.44 ± 0.05	0.17 ± 0.05	1.736 ± 0.017	15.84 ± 0.46	0.27 ± 0.04	0.037 ± 0.002	4.071 ± 0.044	32.3 ± 0.9
13.059 ± 0.131	50.77 ± 0.84	1.016 ± 0.024	14.17 ± 0.24	8.11 ± 0.08	0.25 ± 0.06	3.340 ± 0.033	27.30 ± 0.59	0.33 ± 0.04	0.062 ± 0.003	7.513 ± 0.075	62.8 ± 1.5
12.609 ± 0.126	50.75 ± 0.84	0.995 ± 0.023	13.64 ± 0.23	7.92 ± 0.08	0.27 ± 0.06	3.202 ± 0.032	24.45 ± 0.58	0.39 ± 0.04	0.058 ± 0.003	7.387 ± 0.074	58.2 ± 1.4
12.835 ± 0.128	49.78 ± 0.83	0.923 ± 0.022	16.29 ± 0.26	7.79 ± 0.08	0.28 ± 0.06	3.259 ± 0.033	28.05 ± 0.58	0.51 ± 0.04	0.067 ± 0.003	6.900 ± 0.069	58.3 ± 1.4
6.891 ± 0.069	26.75 ± 0.59	0.520 ± 0.014	8.82 ± 0.17	4.30 ± 0.04	0.11 ± 0.04	1.752 ± 0.018	16.14 ± 0.44	0.17 ± 0.03	0.037 ± 0.002	3.846 ± 0.042	33.1 ± 0.9
6.505 ± 0.065	26.06 ± 0.58	0.496 ± 0.014	9.06 ± 0.17	4.06 ± 0.04	0.15 ± 0.04	1.624 ± 0.016	14.82 ± 0.43	0.14 ± 0.03	0.034 ± 0.002	3.634 ± 0.040	30.7 ± 0.9
4.855 ± 0.049	22.98 ± 0.53	0.352 ± 0.011	3.03 ± 0.10	2.64 ± 0.03	0.11 ± 0.03	1.220 ± 0.013	6.81 ± 0.34	0.13 ± 0.03	0.022 ± 0.002	2.688 ± 0.033	25.2 ± 0.8
4.167 ± 0.042	20.65 ± 0.54	0.329 ± 0.010	2.19 ± 0.08	2.48 ± 0.02	0.09 ± 0.03	1.064 ± 0.012	5.46 ± 0.33	0.08 ± 0.03	0.013 ± 0.002	2.483 ± 0.031	20.2 ± 0.7
3.520 ± 0.035	20.20 ± 0.52	0.278 ± 0.008	1.61 ± 0.07	2.01 ± 0.02	0.13 ± 0.03	0.902 ± 0.011	3.90 ± 0.30	0.07 ± 0.03	0.009 ± 0.002	2.181 ± 0.029	17.4 ± 0.6
4.782 ± 0.048	23.47 ± 0.55	0.340 ± 0.010	1.97 ± 0.08	2.61 ± 0.03	0.08 ± 0.03	1.223 ± 0.013	5.99 ± 0.32	0.08 ± 0.03	0.017 ± 0.002	2.623 ± 0.032	24.2 ± 0.7
6.091 ± 0.061	28.13 ± 0.63	0.409 ± 0.011	2.92 ± 0.09	3.20 ± 0.03	0.08 ± 0.03	1.572 ± 0.016	9.03 ± 0.37	0.12 ± 0.03	0.026 ± 0.002	3.155 ± 0.036	30.4 ± 0.9
4.699 ± 0.047	21.77 ± 0.56	0.322 ± 0.010	2.21 ± 0.08	2.53 ± 0.03	0.05 ± 0.03	1.220 ± 0.013	5.51 ± 0.33	0.08 ± 0.03	0.016 ± 0.002	2.553 ± 0.032	24.2 ± 0.8
3.919 ± 0.039	18.74 ± 0.55	0.278 ± 0.008	2.52 ± 0.09	2.43 ± 0.02	0.09 ± 0.03	1.020 ± 0.012	5.48 ± 0.33	0.09 ± 0.03	0.016 ± 0.002	2.264 ± 0.030	19.8 ± 0.7
3.745 ± 0.037	18.38 ± 0.53	0.272 ± 0.008	2.06 ± 0.08	2.19 ± 0.02	0.10 ± 0.03	0.965 ± 0.011	4.51 ± 0.31	0.07 ± 0.03	0.011 ± 0.002	2.141 ± 0.029	18.7 ± 0.7
3.576 ± 0.036	19.25 ± 0.52	0.260 ± 0.008	1.74 ± 0.07	2.06 ± 0.02	0.05 ± 0.02	0.929 ± 0.011	4.06 ± 0.29	0.04 ± 0.03	0.012 ± 0.002	2.114 ± 0.029	17.3 ± 0.7
3.515 ± 0.035	18.57 ± 0.52	0.262 ± 0.008	1.76 ± 0.07	2.00 ± 0.02	0.10 ± 0.03	0.907 ± 0.011	3.12 ± 0.30	0.03 ± 0.03	0.008 ± 0.002	2.108 ± 0.027	18.3 ± 0.7
2.970 ± 0.030	17.38 ± 0.49	0.255 ± 0.007	1.98 ± 0.08	1.78 ± 0.02	0.07 ± 0.03	0.783 ± 0.010	3.17 ± 0.28	0.06 ± 0.02	0.009 ± 0.002	2.011 ± 0.026	14.8 ± 0.6
2.910 ± 0.029	16.72 ± 0.53	0.260 ± 0.010	1.16 ± 0.06	1.67 ± 0.02	0.06 ± 0.03	0.762 ± 0.010	2.31 ± 0.30	0.01 ± 0.03	0.011 ± 0.002	2.028 ± 0.030	15.0 ± 0.7
3.071 ± 0.031	17.84 ± 0.43	0.281 ± 0.007	1.70 ± 0.07	1.78 ± 0.02	0.09 ± 0.03	0.797 ± 0.010	2.28 ± 0.26	0.02 ± 0.02	0.012 ± 0.002	2.078 ± 0.025	16.1 ± 0.5
3.062 ± 0.031	19.24 ± 0.55	0.273 ± 0.010	1.33 ± 0.07	1.72 ± 0.02	0.06 ± 0.03	0.769 ± 0.010	2.71 ± 0.30	0.05 ± 0.03	0.009 ± 0.002	2.144 ± 0.031	14.1 ± 0.7
3.379 ± 0.034	20.36 ± 0.44	0.316 ± 0.007	1.29 ± 0.06	1.83 ± 0.02	0.07 ± 0.03	0.857 ± 0.010	2.42 ± 0.26	0.04 ± 0.02	0.010 ± 0.002	2.306 ± 0.026	17.5 ± 0.5
3.551 ± 0.036	19.38 ± 0.57	0.320 ± 0.011	1.58 ± 0.07	1.88 ± 0.02	0.06 ± 0.03	0.900 ± 0.011	2.66 ± 0.31	0.07 ± 0.03	0.017 ± 0.002	2.336 ± 0.033	17.3 ± 0.7
4.003 ± 0.040	22.71 ± 0.60	0.318 ± 0.011	1.58 ± 0.07	2.07 ± 0.02	0.10 ± 0.03	1.036 ± 0.012	3.35 ± 0.32	0.04 ± 0.03	0.016 ± 0.002	2.576 ± 0.034	20.5 ± 0.8
3.601 ± 0.036	20.02 ± 0.57	0.306 ± 0.011	1.13 ± 0.06	1.90 ± 0.02	0.01 ± 0.03	0.956 ± 0.012	2.66 ± 0.32	0.07 ± 0.03	0.014 ± 0.002	2.387 ± 0.033	18.5 ± 0.7
4.527 ± 0.045	24.89 ± 0.64	0.346 ± 0.012	1.82 ± 0.08	2.30 ± 0.02	0.05 ± 0.03	1.191 ± 0.013	3.16 ± 0.34	0.04 ± 0.03	0.015 ± 0.002	2.756 ± 0.037	24.3 ± 0.9
4.785 ± 0.048	25.57 ± 0.50	0.383 ± 0.010	2.45 ± 0.08	2.44 ± 0.02	0.08 ± 0.03	1.231 ± 0.013	3.87 ± 0.30	0.03 ± 0.03	0.015 ± 0.002	2.819 ± 0.031	23.7 ± 0.6
5.162 ± 0.052	27.42 ± 0.66	0.383 ± 0.013	2.72 ± 0.10	2.62 ± 0.03	0.08 ± 0.03	1.329 ± 0.014	4.01 ± 0.36	0.08 ± 0.03	0.017 ± 0.002	3.045 ± 0.038	27.1 ± 0.9
5.406 ± 0.054	28.70 ± 0.67	0.381 ± 0.013	2.83 ± 0.10	2.78 ± 0.03	0.03 ± 0.04	1.402 ± 0.015	4.02 ± 0.37	0.04 ± 0.03	0.019 ± 0.002	3.126 ± 0.039	27.1 ± 0.9
5.409 ± 0.054	28.22 ± 0.67	0.398 ± 0.014	3.03 ± 0.10	2.80 ± 0.03	0.09 ± 0.04	1.387 ± 0.014	4.40 ± 0.36	0.16 ± 0.03	0.019 ± 0.002	3.107 ± 0.039	27.1 ± 0.9
5.536 ± 0.055	29.35 ± 0.69	0.404 ± 0.014	2.81 ± 0.10	2.91 ± 0.03	0.12 ± 0.04	1.404 ± 0.015	4.44 ± 0.37	0.08 ± 0.03	0.017 ± 0.002	3.161 ± 0.040	27.4 ± 1.0
5.671 ± 0.057	28.85 ± 0.53	0.417 ± 0.011	4.17 ± 0.11	3.09 ± 0.03	0.09 ± 0.03	1.483 ± 0.015	5.01 ± 0.32	0.14 ± 0.03	0.018 ± 0.002	3.189 ± 0.034	29.9 ± 0.7
5.696 ± 0.057	29.73 ± 0.69	0.414 ± 0.014	4.40 ± 0.12	3.12 ± 0.03	0.10 ± 0.04	1.461 ± 0.015	4.39 ± 0.37	0.11 ± 0.03	0.022 ± 0.002	3.202 ± 0.039	29.2 ± 1.0
5.775 ± 0.058	30.85 ± 0.69	0.414 ± 0.014	4.76 ± 0.12	3.19 ± 0.03	0.12 ± 0.04	1.466 ± 0.015	4.71 ± 0.38	0.16 ± 0.03	0.023 ± 0.002	3.233 ± 0.040	29.2 ± 1.0
5.837 ± 0.058	31.58 ± 0.55	0.418 ± 0.011	6.18 ± 0.14	3.37 ± 0.03	0.15 ± 0.04	1.533 ± 0.015	5.77 ± 0.33	0.12 ± 0.03	0.024 ± 0.002	3.182 ± 0.034	29.6 ± 0.7
6.264 ± 0.063	32.10 ± 0.57	0.417 ± 0.011	6.47 ± 0.14	3.61 ± 0.04	0.17 ± 0.04	1.601 ± 0.016	5.61 ± 0.35	0.22 ± 0.03	0.030 ± 0.002	3.219 ± 0.034	31.3 ± 0.7
6.361 ± 0.064	33.05 ± 0.58	0.435 ± 0.011	7.53 ± 0.16	3.68 ± 0.04	0.17 ± 0.04	1.638 ± 0.016	5.50 ± 0.36	0.20 ± 0.03	0.035 ± 0.002	3.197 ± 0.034	32.7 ± 0.7
6.086 ± 0.061	31.20 ± 0.57	0.396 ± 0.011	7.74 ± 0.16	3.64 ± 0.04	0.22 ± 0.04	1.568 ± 0.016	5.48 ± 0.35	0.17 ± 0.03	0.038 ± 0.002	3.032 ± 0.033	31.9 ± 0.7
5.789 ± 0.058	29.57 ± 0.56	0.394 ± 0.011	8.99 ± 0.17	3.56 ± 0.04	0.17 ± 0.04	1.477 ± 0.015	5.21 ± 0.35	0.24 ± 0.03	0.040 ± 0.002	2.908 ± 0.032	29.3 ± 0.7
5.689 ± 0.057	28.26 ± 0.54	0.372 ± 0.010	7.97 ± 0.16	3.39 ± 0.03	0.22 ± 0.04	1.442 ± 0.014	5.75 ± 0.34	0.31 ± 0.03	0.035 ± 0.002	2.793 ± 0.032	27.8 ± 0.7
5.476 ± 0.055	27.84 ± 0.54	0.362 ± 0.010	7.77 ± 0.15	3.10 ± 0.03	0.17 ± 0.04	1.383 ± 0.014	5.56 ± 0.34	0.22 ± 0.03	0.036 ± 0.002	2.762 ± 0.031	28.6 ± 0.7
5.147 ± 0.051	26.42 ± 0.53	0.327 ± 0.008	6.55 ± 0.14	2.87 ± 0.03	0.23 ± 0.04	1.295 ± 0.013	4.70 ± 0.33	0.27 ± 0.03	0.036 ± 0.002	2.639 ± 0.030	26.2 ± 0.6
3.495 ± 0.035	20.51 ± 0.47	0.275 ± 0.007	4.53 ± 0.11	2.48 ± 0.02	0.13 ± 0.04	0.892 ± 0.011	3.59 ± 0.30	0.15 ± 0.03	0.030 ± 0.002	2.108 ± 0.025	17.4 ± 0.5
3.498 ± 0.035	19.03 ± 0.45	0.278 ± 0.007	4.45 ± 0.11	2.10 ± 0.02	0.18 ± 0.04	0.893 ± 0.011	3.29 ± 0.30	0.18 ± 0.03	0.026 ± 0.002	2.151 ± 0.025	19.3 ± 0.5
3.280 ± 0.033	18.70 ± 0.44	0.273 ± 0.007	4.21 ± 0.10	1.69 ± 0.02	0.09 ± 0.03	0.866 ± 0.010	2.99 ± 0.26	0.06 ± 0.02	0.019 ± 0.002	2.090 ± 0.025	17.1 ± 0.5
3.119 ± 0.031	17.71 ± 0.44	0.257 ± 0.006	2.67 ± 0.08	1.49 ± 0.01	0.17 ± 0.03	0.806 ± 0.010	2.14 ± 0.27	0.08 ± 0.02	0.014 ± 0.002	1.947 ± 0.024	15.9 ± 0.5
2.714 ± 0.027	16.01 ± 0.40	0.235 ± 0.006	2.88 ± 0.08	1.26 ± 0.01	0.07 ± 0.03	0.681 ± 0.009	2.04 ± 0.24	0.05 ± 0.02	0.014 ± 0.002	1.815 ± 0.023	14.0 ± 0.5
2.803 ± 0.028	16.46 ± 0.41	0.243 ± 0.006	1.82 ± 0.07	1.28 ± 0.01	0.08 ± 0.02	0.711 ± 0.009	2.42 ± 0.24	0.02 ± 0.02	0.011 ± 0.002	1.866 ± 0.023	13.2 ± 0.5
2.943 ± 0.029	16.16 ± 0.43	0.228 ± 0.006	2.09 ± 0.07	1.37 ± 0.01	0.02 ± 0.03	0.748 ± 0.009	2.52 ± 0.26	0.06 ± 0.02	0.014 ± 0.002	1.756 ± 0.023	14.9 ± 0.5
2.729 ± 0.027	14.56 ± 0.41	0.228 ± 0.006	1.88 ± 0.07	1.28 ± 0.01	0.07 ± 0.03	0.681 ± 0.009	2.21 ± 0.25	0.05 ± 0.02	0.014 ± 0.002	1.715 ± 0.022	13.6 ± 0.5
2.478 ± 0.025	14.73 ± 0.49	0.215 ± 0.008	1.59 ± 0.07	1.22 ± 0.01	0.04 ± 0.02	0.629 ± 0.009	1.82 ± 0.27	0.04 ± 0.02	0.012 ± 0.002	1.689 ± 0.026	13.0 ± 0.7
2.761 ± 0.028	15.54 ± 0.51	0.221 ± 0.008	1.89 ± 0.07	1.25 ± 0.01	0.05 ± 0.03	0.697 ± 0.009	2.00 ± 0.28	0.01 ± 0.02	0.015 ± 0.002	1.768 ± 0.026	14.9 ± 0.7
3.014 ± 0.030	16.43 ± 0.52	0.227 ± 0.008	2.25 ± 0.08	1.35 ± 0.01	0.07 ± 0.03	0.756 ± 0.010	2.35 ± 0.28	0.08 ± 0.03	0.011 ± 0.002	1.815 ± 0.027	17.8 ± 0.7
2.869 ± 0.029	16.03 ± 0.52	0.226 ± 0.008	2.23 ± 0.08	1.26 ± 0.01	0.06 ± 0.03	0.719 ± 0.009	2.36 ± 0.29	0.05 ± 0.02	0.014 ± 0.002	1.751 ± 0.026	14.6 ± 0.7
2.728 ± 0.027	14.78 ± 0.50	0.214 ± 0.008	1.59 ± 0.07	1.19 ± 0.01	0.39 ± 0.05	0.667 ± 0.009	2.56 ± 0.27	0.04 ± 0.02	0.017 ± 0.002	1.684 ± 0.025	14.4 ± 0.7
2.534 ± 0.025	14.95 ± 0.50	0.198 ± 0.008	1.43 ± 0.07	1.21 ± 0.01	0.10 ± 0.03	0.639 ± 0.009	1.97 ± 0.27	0.07 ± 0.02	0.009 ± 0.002	1.629 ± 0.025	14.6 ± 0.7
2.579 ± 0.026	13.68 ± 0.50	0.200 ± 0.008	1.44 ± 0.06	1.18 ± 0.01	0.02 ± 0.02	0.654 ± 0.009	2.25 ± 0.26	0.11 ± 0.02	0.011 ± 0.002	1.609 ± 0.025	13.5 ± 0.7
2.619 ± 0.026	15.24 ± 0.51	0.191 ± 0.007	1.06 ± 0.06	1.19 ± 0.01	0.01 ± 0.02	0.642 ± 0.009	1.84 ± 0.27	0.05 ± 0.02	0.009 ± 0.002	1.589 ± 0.025	14.1 ± 0.7
		0.192 ± 0.005	1.01 ± 0.05	1.13 ± 0.01	0.03 ± 0.02	0.644 ± 0.009	1.44 ± 0.26	0.02 ± 0.02	0.010 ± 0.002	1.563 ± 0.021	12.6 ± 0.4
		0.215 ± 0.006	1.66 ± 0.07	1.14 ± 0.01	0.06 ± 0.02	0.784 ± 0.010	2.05 ± 0.26	0.08 ± 0.02	0.010 ± 0.002	1.646 ± 0.022	15.8 ± 0.4
		0.220 ± 0.006	1.22 ± 0.06	1.15 ± 0.01	0.01 ± 0.02	0.721 ± 0.009	2.62 ± 0.25	0.03 ± 0.02	0.012 ± 0.002	1.736 ± 0.022	15.5 ± 0.4
		0.215 ± 0.006	1.35 ± 0.06	1.25 ± 0.01	0.00 ± 0.02	0.731 ± 0.010	2.23 ± 0.25	0.00 ± 0.02	0.032 ± 0.002	1.624 ± 0.021	15.6 ± 0.4
		0.219 ± 0.006	1.51 ± 0.06	1.24 ± 0.01	0.02 ± 0.02	0.723 ± 0.010	3.06 ± 0.25	0.03 ± 0.02	0.011 ± 0.002	1.720 ± 0.022	15.5 ± 0.4
		0.236 ± 0.006	1.52 ± 0.06	1.28 ± 0.01	0.04 ± 0.02	0.782 ± 0.010	2.85 ± 0.26	0.06 ± 0.02	0.013 ± 0.002	1.781 ± 0.023	15.8 ± 0.4
		0.242 ± 0.006	1.55 ± 0.07	1.41 ± 0.01	0.09 ± 0.03	0.890 ± 0.011	2.74 ± 0.27	0.03 ± 0.02	0.013 ± 0.002	1.845 ± 0.023	18.4 ± 0.5
		0.247 ± 0.006	1.52 ± 0.06	1.40 ± 0.01	0.03 ± 0.02	0.792 ± 0.010	2.99 ± 0.26	0.03 ± 0.02	0.009 ± 0.002	1.885 ± 0.023	16.3 ± 0.4
		0.237 ± 0.006	2.24 ± 0.08	1.55 ± 0.02	0.10 ± 0.03	0.845 ± 0.010	3.54 ± 0.26	0.04 ± 0.02	0.014 ± 0.002	1.830 ± 0.023	16.8 ± 0.4
		0.280 ± 0.007	2.27 ± 0.08	1.73 ± 0.02	0.07 ± 0.03	0.919 ± 0.011	3.36 ± 0.26	0.06 ± 0.02	0.012 ± 0.002	2.121 ± 0.024	18.8 ± 0.5
		0.287 ± 0.007	2.75 ± 0.09	1.99 ± 0.02	0.08 ± 0.03	1.116 ± 0.012	4.58 ± 0.28	0.05 ± 0.02	0.015 ± 0.002	2.235 ± 0.025	21.9 ± 0.5
		0.855 ± 0.018	22.11 ± 0.29	6.00 ± 0.06	0.31 ± 0.06	5.456 ± 0.055	29.22 ± 0.54	0.46 ± 0.04	0.080 ± 0.003	6.961 ± 0.070	106.6 ± 16.0
		0.318 ± 0.008	3.67 ± 0.10	2.07 ± 0.02	0.06 ± 0.03	1.220 ± 0.013	4.45 ± 0.29	0.08 ± 0.03	0.020 ± 0.002	2.467 ± 0.027	24.5 ± 0.5
		0.250 ± 0.007	2.18 ± 0.08	1.59 ± 0.02	0.04 ± 0.02	0.927 ± 0.011	2.91 ± 0.25	0.04 ± 0.02	0.012 ± 0.002	1.979 ± 0.024	19.8 ± 0.5
		0.255 ± 0.007	2.40 ± 0.08	1.58 ± 0.02	0.10 ± 0.03	0.953 ± 0.011	3.52 ± 0.26	0.04 ± 0.02	0.015 ± 0.002	1.985 ± 0.024	19.4 ± 0.5
		0.316 ± 0.008	3.73 ± 0.10	1.82 ± 0.02	0.09 ± 0.03	1.283 ± 0.013	4.59 ± 0.29	0.09 ± 0.03	0.017 ± 0.002	2.462 ± 0.027	26.4 ± 0.6
		0.280 ± 0.007	1.69 ± 0.07	1.34 ± 0.01	0.04 ± 0.02	0.830 ± 0.010	2.61 ± 0.25	0.05 ± 0.02	0.012 ± 0.002	2.099 ± 0.024	16.5 ± 0.4

peaks in Section 4 (Peak B at 110 cm, Peak C at 81–83 cm, Peak D at 77–78 cm) have Ir/Fe ratios that are one to two orders of magnitude higher than background (Fig. 1), and they should, therefore, have a different origin. The elevated tail in the lower part of Section 4 is also not likely to be due to background (Fig. 1).

The rise of the main Ir peak is steepest between Samples 577B-1-4, 74 cm and 577B-1-4, 73 cm, which is in close agreement with the location of the Cretaceous/Tertiary boundary at 577B-1-4, 72 cm defined by nannofossil studies (Site 577 chapter, this volume; Monechi, this volume). Similar agreements between biostratigraphic and geochemically defined Cretaceous/Tertiary boundary levels (Asaro et al., 1982) have been found in many marine sections, and these would be expected from the asteroid-impact theory. The three smaller peaks below the main peak (Peaks B, C, and D in Fig. 1) and the elevated tail, however, should not be primary deposits in Cretaceous sediment if the asteroid-impact theory is correct.

Bioturbation can cause smearing of sharp boundaries, but it is not clear that it would produce the two well-shaped peaks (C and D) seen in Figure 1. Also the

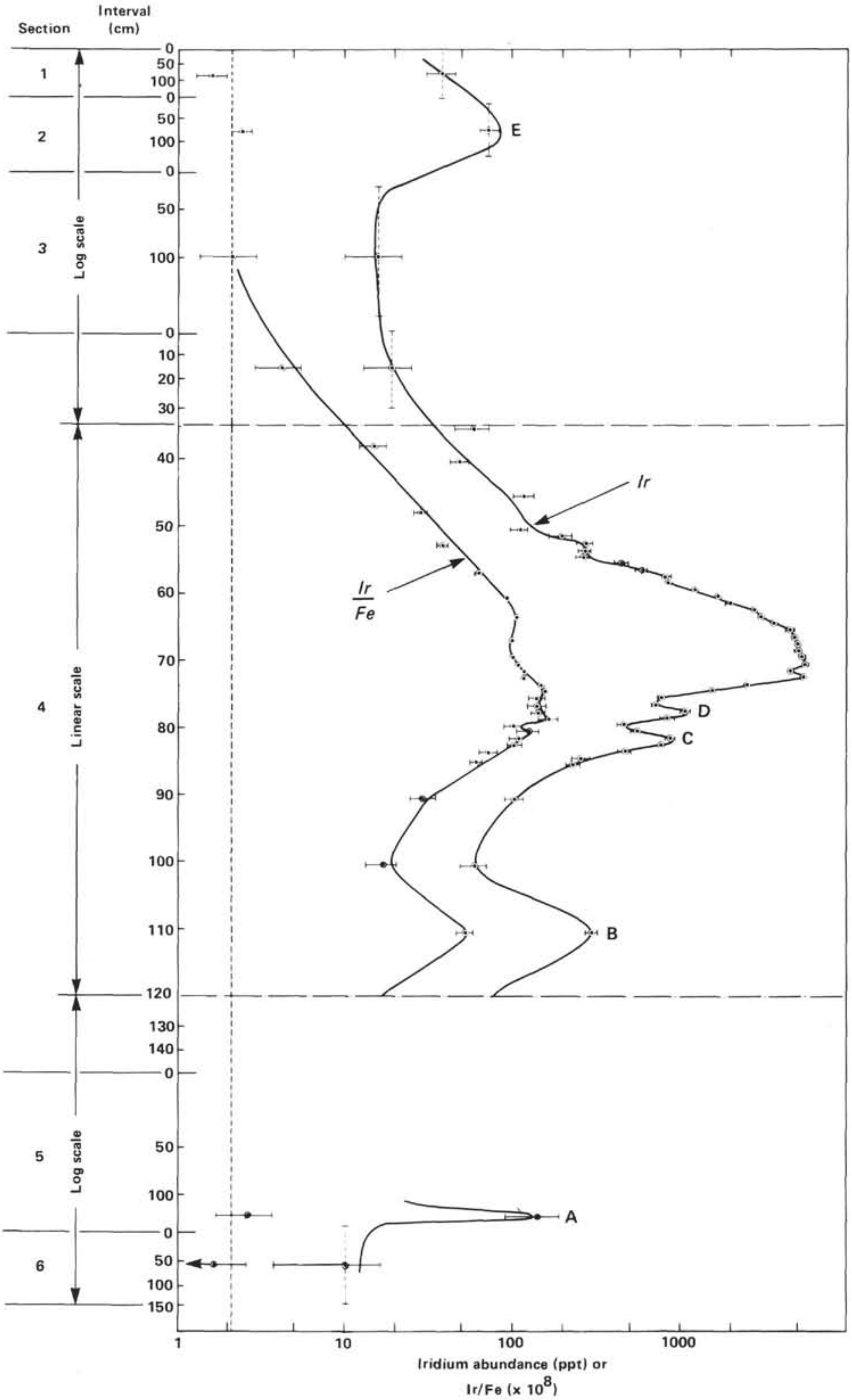

Figure 1. Stratigraphic position in Core 577B-1 versus abundance of iridium (ppt) and (Ir/Fe) $\times 10^{-8}$. The main Ir anomaly is located between 65 and 73 cm in Section 4. Five smaller anomalies, labeled A–E occur in Samples 577B-1-5, 120–121 cm (Peak A) 577B-1-4, 110–111 cm (Peak B), 577B-1-4, 81–83 cm (Peak C), 577-1-4, 77–78 cm (Peak D) and 577B-1-1, 10 cm to 577B-1-2, 121 cm (Peak E). The depth over which a sample was collected for the Ir measurements is shown by a vertical bar. A dashed vertical bar indicates the collection was not continuous.

extent of penetration of the tail into the Cretaceous sediment (over a meter) and the depth of Peak B below the main Ir distribution (38 cm) are greater than would be expected from bioturbation. Iridium in Cretaceous/Tertiary sediments is to some extent soluble in acids (L. W. Alvarez et al., 1980) and the observed tail may be due to mobility of the Ir. It is also possible that Peak B is due to contamination or to another impact (Davis et al., 1984, Whitmire and Jackson, 1984). A method of checking some of these suppositions would be to resample the material below the sliced surface. As neither bioturbation nor contamination is likely to reproduce Peaks B, C, and D in measurements of such samples, another cause would be likely if the peaks are still observed.

Siderophile Element Abundances

Cobalt, Ni, Cr, and Fe all show abundance profiles similar to that of Ir (Table 1) near the Cretaceous/Tertiary boundary, as do the lithophile elements Al and Ta (Fig. 3). The Ni/Ir ratio is about a factor of 3 lower than the chondritic value and the Cr/Ir ratio is about a factor of 1.5 lower.

At Stevns Klint, Denmark and at Deep Sea Drilling Project (DSDP) Hole 465A in the Central Pacific Ocean, siderophile elements measured have ratios consistent with mixtures of terrestrial and meteoritic (chondritic) components (F. Asaro, W. Alvarez, H. V. Michel, L. W. Alvarez, M. Kastner, and J. Thiede, unpubl. data). The anoxic environment in which sediments from these sections were deposited may have preserved the ratios of these siderophile elements, as these elements form insoluble sulfides.

Sulfur was not measured in the Hole 577B sediments. As none of the sediments contain measurable amounts of Se (<0.7 ppm), which is normally associated with sulfide deposits, the environment of deposition at Site 577 was probably not anoxic, and some siderophile elements may have been lost during diagenesis.

Rare-Earth Patterns

Hole 577B rare-earth element abundance patterns divided by the chondritic values (Masuda et al., 1973) are shown in Figure 2. The large negative Ce anomaly (characteristic of seawater) indicates that the predominant rare-earth elements were originally dissolved in seawater. As seen in Figure 3, Ce (over and above the amount that is associated with Sm in the region directly above and below the boundary) has the same abundance profile as Ir in the boundary region. This excess Ce may be due to a detrital component from the impact site. In addition to excess Ce, the ratio of heavy to light rare-earth elements is smaller in the Ir-rich region than above and below this region.

DISCUSSION

Sedimentation Rate

Barker and Anders (1968) measured the content of Ir in Pacific red clays as a maximum of 140 ppt, for a deposition rate of 1 mm per thousand years and a density of 0.5 g of solid per cubic centimeter of wet sediment.

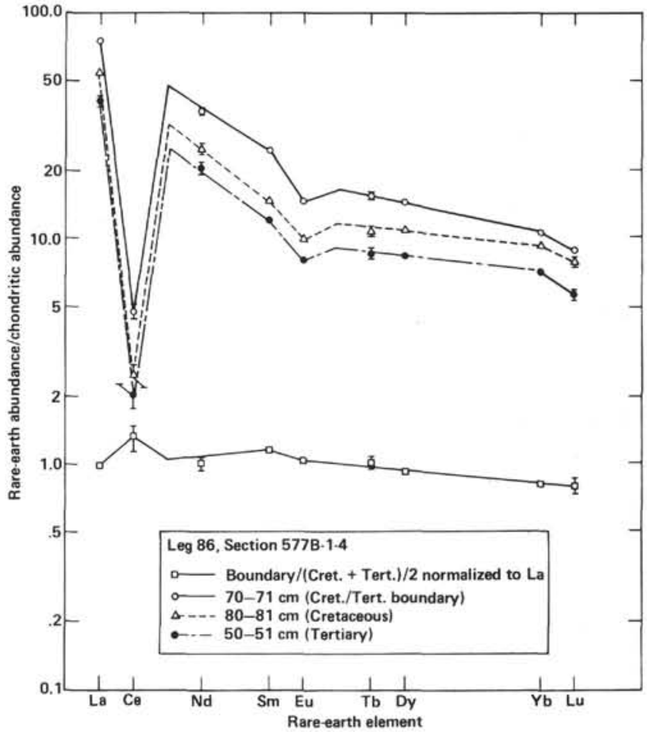

Figure 2. Rare-earth element abundances divided by those of Leedy chondrite (Masuda et al., 1973) as a function of atomic number.

About half of this Ir was attributed to an extraterrestrial source and half to sources independent of the deposition rate, but the uncertainties were such that all of the Ir could have come from the extraterrestrial source. Kyte and Wasson (1982) found a somewhat higher abundance of Ir, when normalized to the same deposition rate. With the Barker and Anders (1968) maximum Ir deposition value, a 1.9 m/m.y. average sedimentation rate given in the Site 577 chapter (this volume) for the Cretaceous/Tertiary boundary region, and a density of 0.8 g/cm^3, the background Ir should be about 46 ppt. This is consistent with the present work as it is about midway between the highest (73 ppt) and lowest (10 ppt) values of the measured Ir background. Assuming the Barker and Anders (1968) maximum meteorite Ir deposition rate and a density of 0.8 g/cm^3, the rate of sedimentation at any stratigraphic level in this section, where the "background" Ir abundance from normal meteoritic dust can be measured, would therefore be 46 (m/m.y.)/background Ir abundance (ppt).

Integrated Amount of Ir

If the products of the Ir abundance in each stratigraphic interval and the stratigraphic height of the interval are summed over the boundary region, and a background of 0.015 ppb times the total stratigraphic height is removed, and the net value is multiplied by a density of 0.8 g/cm^3, there are found to be 61 ng/cm^2 of anomalous Ir in the boundary region. This is comparable to the average amount found at other studied Cretaceous/Tertiary sections worldwide (50 ng/cm^2) (W. Alvarez et al., 1982b).

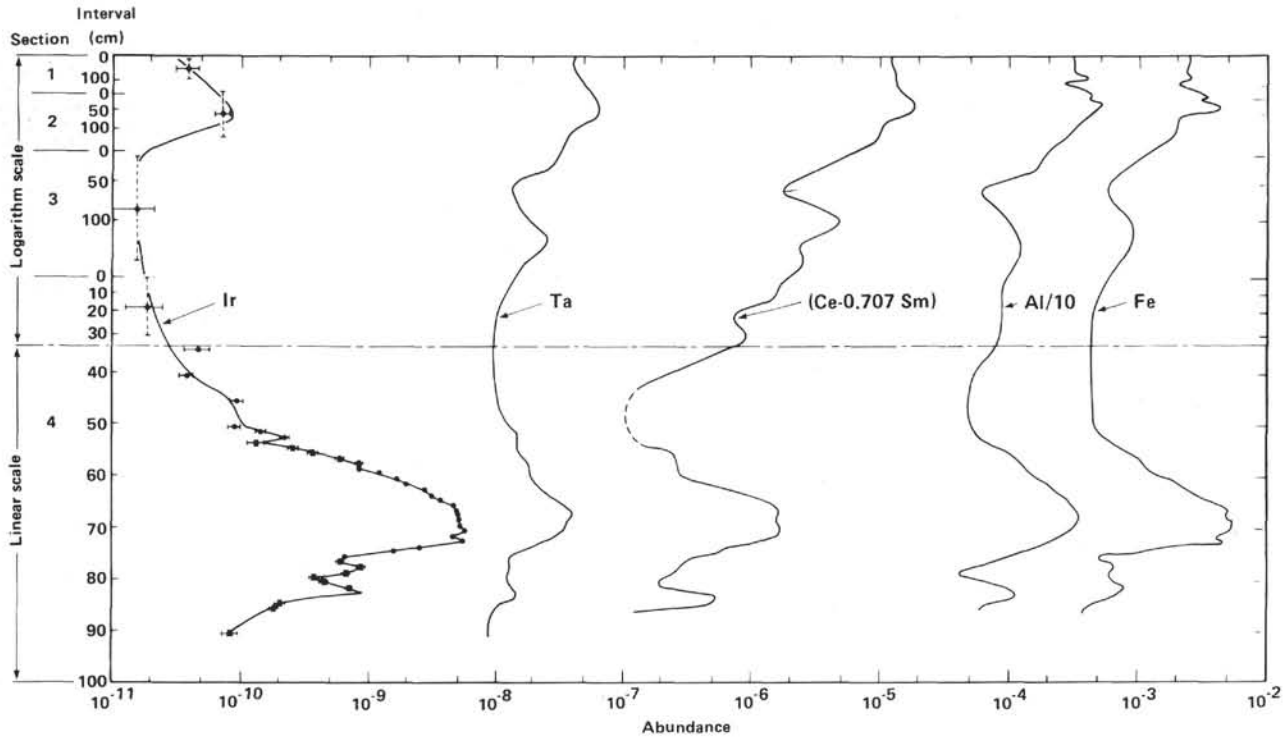

Figure 3. Abundances of Ir, Ta, (Ce − 0.707Sm), Al/10 and Fe as a function of stratigraphic position in Core 577B-1, Shatsky Rise.

CONCLUSION

The Ir anomaly predicted by the asteroid-impact theory was found in the Cretaceous/Tertiary boundary region of Hole 577B and its magnitude was 61 ng/cm^2. The sharp rise of the main Ir peak occurs within 2 cm of the Cretaceous/Tertiary boundary as defined by nannoplankton (Monechi, this volume). Five other small Ir peaks as well as an elevated tail are also observed near the main Ir peak. Two of the small peaks are probably related to changes in the $CaCO_3$ deposition rate, while two others and the elevated tail may be due to perturbations of the main peak. One small Ir peak remains unexplained. Siderophile element (Cr/Ir and Ni/Ir) ratios are somewhat different from chondritic values in the Cretaceous/Tertiary region, but this may be due to loss of elements in the oxidizing marine environment.

ACKNOWLEDGMENTS

We are grateful to Audrey Wright and Amy Altman for their assistance in obtaining the samples, to Audrey Wright for her help in editing the manuscript, and to Charles J. Orth and Frank T. Kyte for reviewing the manuscript. We thank Tek Lim and his staff at the Berkeley Triga Reactor for the neutron irradiations. We also appreciate the assistance of Raphael Zamora and Jon Bechtel in sample preparation and data reduction. Jonathan Stebbins was most helpful in the development of the high-temperature Ir separations.

Funding for this work was provided by the Director, Office of Energy Research, Office of Basic Sciences Division of Engineering, Mathematical and Geosciences of U.S. Department of Energy under Contract No. DE-AC03-76SF00098, the U.S. National Science Foundation under Grant EAR-81-15858, and the National Aeronautics and Space Administration Ames Research Center under Contract A-71683B. DSDP samples were provided through the assistance of the National Science Foundation.

REFERENCES

Alvarez, L. W., Alvarez, W., Asaro, F., and Michel, H. V., 1980. Extraterrestrial cause for the Cretaceous-Tertiary extinction. *Science*, 208:1095–1108.

Alvarez, W., Alvarez, L. W., Asaro, F., and Michel, H. V., 1982a. Iridium anomaly approximately synchronous with terminal Eocene extinctions. *Science*, 216:868–888.

________, 1982b. Current status of impact theory for the terminal Cretaceous extinction. *Spec. Pap. Geol. Soc. Am.*, 190:305–315.

________, 1984. The end of the Cretaceous: Sharp boundary or gradual transition. *Science*, 223:1183–1186.

Asaro, F., Alvarez, L. W., Michel, H. V., and Alvarez, W., 1982. Letter to Editor. *Am. Sci.*, 70:567–568.

Barker, J. L., and Anders, E., 1968. Accretion rate of cosmic matter from iridium and osmium contents of deep sea sediments. *Geochim. Cosmochim. Acta*, 32:627–645.

Davis, M., Hut, P., and Muller, R. A., 1984. Extinctions of species by periodic comet showers. *Nature*, 308:715–717.

Kyte, F., and Wasson, J. T., 1982. A search for iridium anomalies in sediments deposited during the past 70 Ma. *Lunar Planet. Sci.*, XIII:411–412. (Abstract)

Masuda, A., Nakamura, N., Tanaka, T., 1973. Fine structures of mutually normalized rare-earth patterns of chondrites. *Geochim. Cosmochim. Acta*, 37:239–248.

Perlman, I., and Asaro, F., 1969. Pottery analysis by neutron activation. *Archaeometry*, 11:21–52.

________, 1971. Pottery analysis by neutron activation. *In* Brill, R. H. (Ed.), *Science and Archaeology*: Cambridge (M.I.T. Press), pp. 182–195.

Rammensee, W., and Palme, H., 1982. "Metal-silicate extraction technique for the analysis of geological and meteoritic samples." *J. Radioanal. Chem.*, 71:401–418.

Whitmire, D. P., and Jackson, A. A., IV, 1984. Are periodic mass extinctions driven by a distant solar companion? *Nature*, 308: 713–715.

Date of Initial Receipt: 30 January 1984
Date of Acceptance: 6 June 1984